Optical study of $Ba(Mn_xTi_{(1-x)}O_3)$ thin films by spectroscopic ellipsometry*

Zhang Ting(张 婷)[a)b)], Yin Jiang(殷 江)[a)], Ding Ling-Hong(丁玲红)[b)], and Zhang Wei-Feng(张伟风)[b)†]

[a)] National Laboratory of Solid State Microstructures, Nanjing University, Nanjing 210093, China

[b)] Key Laboratory of Photovoltaic Materials of Henan Province, School of Physics and Electronics, Henan University, Kaifeng 475004, China

(Received 21 March 2013; revised manuscript received 28 May 2013)

Stoichiometric $Ba(Mn_xTi_{(1-x)}O_3)$ (BMT) thin films with various values of x were deposited on Si(111) substrates by the sol-gel technique. The influence of Mn content on the optical properties was studied by spectroscopic ellipsometry (SE) in the UV–Vis–NIR region. By fitting the measured ellipsometric parameter (Ψ and Δ) with a four-phase model (air/BMT+voids /BMT/Si(111)), the key optical constants of the thin films have been obtained. It was found that the refractive index n and the extinction coefficient k increase with increasing Mn content due to the increase in the packing density. Furthermore, a strong dependence of the optical band gap E_g on Mn/Ti ratios in the deposited films was observed, and it was inferred that the energy level of conduction bands decreases with increasing Mn content.

Keywords: $Ba(Mn_xTi_{(1-x)}O_3)$ (BMT) thin films, spectroscopic ellipsometry, refractive index, extinction coefficient

PACS: 78.20.Bh, 78.20.Ci, 78.66.–w, 78.68.+m **DOI:** 10.1088/1674-1056/22/11/117801

1. Introduction

Perovskite ferroelectric materials have attracted considerable attention for a wide range of applications, such as dynamic random access memories (DRAMs), microwave tunable phase shifters, second harmonic generators (SHGs), electro-optic switches, pyroelectric detectors, optical modulators, and mixers.[1–3] Among these materials, $BaTiO_3$ is a typical ferroelectric material and considered to be very promising for optical information processing and storage.[4,5] Furthermore, element doping has a great effect on the physical properties of ferroelectric materials.[6–11] This offers an approach through which the properties of materials can be modified by selecting a proper element as the dopant. Optimal cation doping (Ti^{4+}) is a widely accepted approach to tailor the physical properties, such as transition temperature, ferroelectric characteristics, and dielectric properties. There has been an increased interest in transition metal (TM) doped wide-band-gap materials, which was amplified by theoretical predictions suggesting that ferromagnetism of diluted magnetic compounds with Curie temperatures above room temperature (RT) can be obtained.[12] The manganese (Mn) element is a typical TM and its doping can produce some perturbation on the physical properties in the ferroelectric materials.[8,10] Therefore, it is interesting and significant to investigate the optical properties of Mn-doped $BaTiO_3$ films due to the unique characteristics by the replacement of Ti^{4+}.

Spectroscopic ellipsometry (SE), which is very sensitive to ultrathin films and surfaces, is a novel, nondestructive, and powerful technique to investigate the optical characteristics of materials, and particularly to measure simultaneously the thickness and the dielectric function of a multilayer system.[13–16] Recently, researchers reported the infrared optical properties of $BaTiO_3$ thin films using spectroscopic ellipsometry.[5,17,18] In their work, however, the measured wavelength range is only in the infrared range. Up to now, there is little data on the optical constant spectra of doping $BaTiO_3$ thin films in a wide wavelength range. The investigations of the UV–Vis–NIR optical properties of doped $BaTiO_3$ thin films are of particular importance for, e.g., optical modulation and optical display devices.

In this paper, we report on the SE measurements of the key optical constants for $Ba(Mn_xTi_{(1-x)}O_3)$ (BMT) thin films in the UV–Vis–NIR range, and the main objective is to determine the optical properties of BMT thin films as a function of their compositions.

2. Experimental details

In this work, BMT thin films with various values of x ($x = 0$, 0.01, 0.02, 0.05, and 0.10) were prepared on Si(111) substrates by the sol-gel method. High-purity barium acetate $[Ba(CH_3COO)_2]$, manganesel acetate $[Mn(CH_3COO)_24H_2O]$, and tetrabutyl titanate $[Ti(OC_4H_9)_4]$ were used as starting materials. 2-methoxyethnaol ($CH_3OCH_2CH_2OH$) and acetylacetone ($CH_3COCH_2COCH_3$) were used as the solvent and the chemical modifier, respectively. It should be emphasized that all

*Project supported by the National Natural Science Foundation of China (Grant No. 60976016), the Postdoctoral Science Foundation of China (Grant No. 2012M511250), and the Foundation Co-established by Henan Province and the Ministry of Henan University, China (Grant No. SBGJ090503).

†Corresponding author. E-mail: wfzhang@henu.edu.cn

© 2013 Chinese Physical Society and IOP Publishing Ltd

chemical materials and organic reagents are analytically pure. Therefore, the effects from impurities in the solution could be neglected, as compared to the Mn doping concentration in the present work. The precursor solution was spin-coated directly on Si(111) substrate to form a uniform wet film at room temperature. The rotation speed and the spin time were fixed at 4000 rpm and 30 s, respectively. Each layer of the wet films was initially dried at 180 °C to evaporate the solvent, and then rapidly heated to 380 °C to remove the residual organics. Finally, the films were annealed at 700 °C. Each section of the rapid thermal treatment was held for 5 min. The spin-coating and thermal treatments were repeated four times.

The crystalline structure of the films was determined by X-ray diffraction (XRD, DX2500) using Cu Kα radiation. The ellipsometric measurements were carried out at room temperature by a variable-angle spectroscopic ellipsometry (V-VASE with Auto Retarder), with a synchronously rotating polarizer in the UV–Vis–NIR region (290–1700 nm, or 0.73–4.28 eV).

3. Results and discussion

Figure 1 shows the XRD patterns of the BMT thin films. Several peaks corresponding to BMT reflection peaks accompanied by Si (111) substrate reflection peaks were observed in the pattern, indicating that the samples are cubic perovskite and no pyrochlore phase exists. This indicates that 700 °C is high enough for the films to be crystallized. We find no obvious shift of the peak positions by comparing the four curves. This means that the changes in the lattice constant caused by different Mn contents are too small to be detected when the Mn content is lower than 0.1. This result is similar to the phenomena observed in $Ba(Ti_{1-x}, Fe_x)O_3$.[19] The average particle size in the samples is estimated from the X-ray line widths given by Scherrer's equation: $D = k\lambda/\beta\cos\theta$, where D is the particle diameter, k is the Scherrer constant (shape factor is about 0.9), λ is the wavelength of X ray, β is the full width at half maximum of the X ray diffraction peak, and θ is the diffraction angle. The average grain size in our samples is 20 nm. In Fig. 1, the Si (111) peaks are absent for the BMT thin films with $x = 0.02$ and $x = 0.10$. This may originate from infinitesimal uneven areas of the samples during the test, resulting in a crystal plane angle which slightly deviates from the exact Bragg angle.

A schematic of the experimental setup is shown in Fig. 2(a). Electromagnetic radiations are emitted by a light source and linearly polarized by a polarizer. It can pass through an optional compensator (retarder, quarter wave plate) and fall onto the sample. After reflection, the radiation passes a compensator (optional) and a second polarizer, which is called an analyzer, and falls into the detector. The system operations, including data acquisition and reduction, preamplifier gain control, incident angle, wavelength setting, and scanning, were fully and automatically controlled by a computer. The incident angle was continuously varied between 20° and 90°.

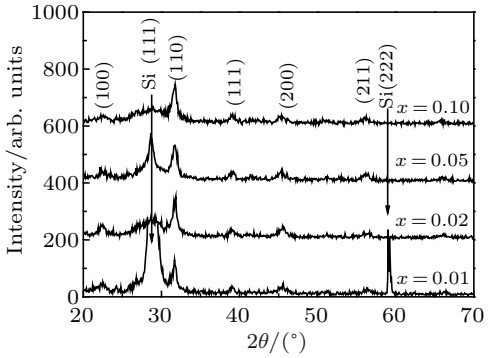


Fig. 1. XRD patterns of BMT thin films deposited on Si (111) substrates annealed at 700 °C for 3 min with rapid thermal annealing (RTA).

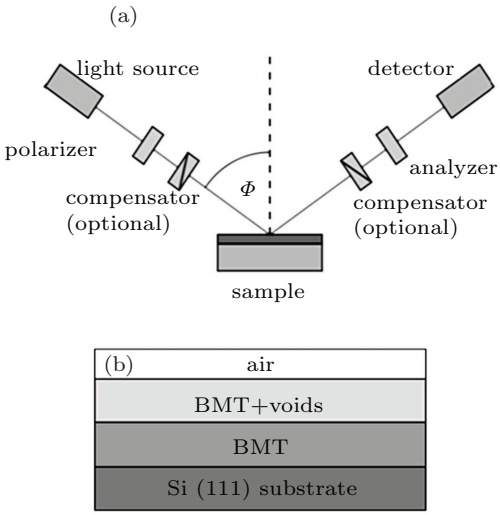


Fig. 2. (a) Schematic images of the experimental setup and (b) the film structure used in the SE fitting.

Ellipsometry measures two of the four Stokes parameters, which are conventionally denoted by Ψ and Δ. The polarization state of the light incident upon the sample may be decomposed into an s and a p component (the s component oscillates in the direction perpendicular to the plane of incidence and parallel to the sample surface, and the p component oscillates in the direction parallel to the plane of incidence). The amplitudes of the s and p components, after reflection and normalization to their initial value, are denoted by r_s and r_p, respectively. Ellipsometry measures the ratio of r_s and r_p, which is described by the fundamental equation of ellipsometry,

$$\rho = \frac{r_p}{r_s} = \tan(\psi)\,e^{i\Delta}. \quad (1)$$

Thus, $\tan\Psi$ is the amplitude ratio upon reflection, and Δ is the phase shift (difference). Since ellipsometry measures the ratio (or difference) of two values (rather than the absolute values), it is very robust, accurate, and reproducible. For instance, it is relatively insensitive to scatter and fluctuations, and requires no standard sample or reference beam.

Commonly, ρ is transformed into the pseudodielectric function $\langle\varepsilon\rangle$ which is given by[20]

$$\begin{aligned}\langle\varepsilon\rangle &= \langle\varepsilon_1\rangle + \mathrm{i}\langle\varepsilon_2\rangle \\ &= \varepsilon_\mathrm{a}\sin^2\phi\left\{1+\tan^2\phi\left[(1-\rho)/(1+\rho)\right]\right\},\end{aligned} \tag{2}$$

where ϕ is the angle of incidence, and ε_a is the dielectric function of the ambient.

The optical functions of a material are usually expressed in terms of the complex refractive index defined as

$$\tilde{n} = n + \mathrm{i}k = \sqrt{\varepsilon}, \tag{3}$$

where n is the refractive index, and k is the extinction coefficient. Meanwhile, the optical constants such as n and k are determined by[18]

$$\begin{aligned}n &= \frac{1}{\sqrt{2}}\sqrt{\sqrt{\varepsilon_1^2+\varepsilon_2^2}+\varepsilon_1}, \\ k &= \frac{1}{\sqrt{2}}\sqrt{\sqrt{\varepsilon_1^2+\varepsilon_2^2}-\varepsilon_1}.\end{aligned} \tag{4}$$

Ellipsometry is an indirect method, which means that in general the measured Ψ and Δ cannot be converted directly into the optical constants of the sample. Normally, a model analysis must be performed. For a layer sample, the measured spectra may be analyzed using an appropriate fitting model, constructed on the basis of the sample structure. Using an iterative procedure (least-squares minimization), unknown optical constants and/or thickness parameters are varied, and Ψ and Δ values are calculated using the Fresnel equations. The calculated Ψ and Δ values, which match the experimental data best, provide the optical constants and thickness parameters of the sample. In our work, the optical constants derived from the ellipsometric parameters of $\tan\Psi$ and $\cos\Delta$ are analyzed by using a four-phase model (air/BMT+voids/BMT/substrate), as shown in Fig. 2(b). The presence of a rough surface layer is a common feature for sol-gel-derived oxide thin films.[21] The rough surface layer was modeled using a Bruggeman effective medium approximation[22] consisting of voids and BMT.

The SE spectra for BMT thin films with x from 0.01 to 0.1 are shown in Fig. 3. In the higher energy range, the spectra exhibit oscillations. This is only due to the interference effect of light, and indicates that the films are transparent. The oscillating frequency depends on the thickness of the film. Generally, the thicker the film is, the higher the frequency is. With the help of simulated annealing optimization,[23] the fitting parameters as well as the film thicknesses were determined by fitting the ellipsometric spectra. Figure 3 also shows the fitting curves for BMT thin films, which exhibits good accordance. Table 1 shows the details of the fitting parameters for four BMT films.

Table 1. The fitted thickness of BMT films with different Mn/Ti ratios determined by SE.

x	BMT+voids/nm	BMT/nm	Si(111)/mm
$x = 0.01$	4.37	299.53	0.5
$x = 0.02$	4.36	299.43	0.5
$x = 0.05$	4.33	296.60	0.5
$x = 0.10$	4.32	293.61	0.5

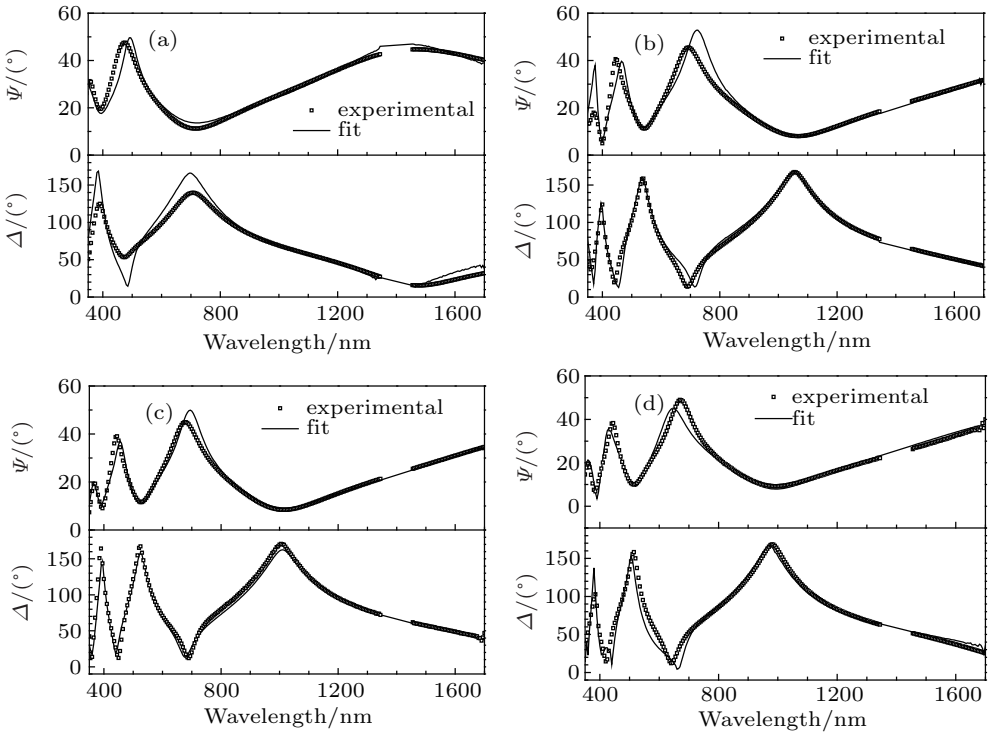


Fig. 3. Ellipsometric spectra of BMT thin films as a function of Ti contents. (a) $x = 0.01$, (b) $x = 0.02$, (c) $x = 0.05$, and (d) $x = 0.10$.

Figure 4 shows the refractive index (n) and extinction coefficient (k) obtained from the fitting parameters for four BMT films. From Fig. 4, we find that the optical constants of all BMT films decrease rapidly in the near-ultraviolet region, and then approach unity (normal dispersion). They show a high refractive index ($n = 1.8$–2.5) in the UV–Vis–NIR region as well as the fundamental absorption edge in the near-ultraviolet region. The n and k agree with the Cauchy scatter expressions and Urbach absorption relations, respectively. In addition, we also find different values of n and k due to different compositions. The refractive index of the BMT films increases with increasing Mn content in the range shown in the inset of Fig. 4. This is the same as PZT ceramics, whose refractive index is largely controlled by the Zr/Ti ratio.[24] When Mn^{4+} is a substitute for Ti^{4+} in the $BaTiO_3$ films, Mn^{4+} ions with small radii ($r = 0.53$ nm) will occupy the lattice site of the Ti^{4+} ions with a big radii ($r = 0.605$ nm), which will enhance the coupling effect between the Ba^{2+} and O^{2-} ions because the effect of the Mn–O bond is stronger than that of the Ti–O bond. A higher Mn content in BMT films enhances the formation of larger and more closely packed crystals. The increase in n with increasing Mn content can be partly attributed to the increase in the packing density. The extinction coefficient (k) spectra for the samples with different Mn contents are also shown in Fig. 4. It is interesting that the extinction coefficient also increases as the Mn content increases. The values of the extinction coefficient, as we know, result from the absorption and grain scattering when the photon wavelength is equivalent to the grain size in the high-energy region. The possibility of scattering of the grains increases as the Mn content increases, which can also be attributed to the increase in grain size and surface density of the films. The extinction coefficient near the fundamental band gap energy is not zero because of the noise, and the results demonstrated that some other types of absorption are present in addition to the fundamental transition. A good agreement is obtained between the experimental and calculated spectra in the measured wavelength range,[25] especially near the fundamental band gap region. Beyond the fundamental optical band gap, there are high-energy critical point transitions. For the $BaTiO_3$ material, they are far away from 4.28 eV and cannot be detected by the present measurements due to the spectral limitation and sensitivity.

The optical absorption coefficient is also a useful parameter and is given by $\alpha = 4\pi k/\lambda$, where λ is the wavelength of light. The dependence of $(h\nu\alpha)^2$ on $h\nu$ of BMT thin films is shown in Fig. 5. In the high-energy region of the absorption edge, $(h\nu\alpha)^2$ varies linearly with $h\nu$, which is taken as the prime evidence for the direct band gap. Based on the above analysis, the relation between absorption coefficient α and the band gap E_g can be described as[26]

$$(h\nu\alpha)^2 = C(h\nu - E_g). \tag{5}$$

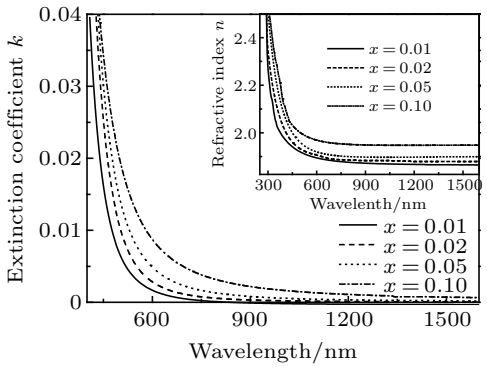


Fig. 4. Optical constants (n and k) of BMT films with different Mn/Ti ratios.

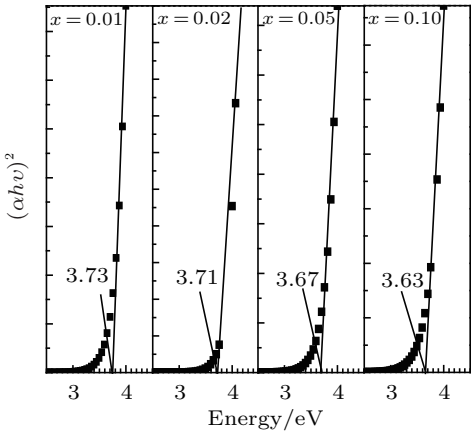


Fig. 5. Optical band gap energies of BMT films as a function of Ti contents (x denotes the content of Mn).

This corresponds to an allowed direct transition between valence and conduction bands. By extrapolating the linear portion of the curves to intersect with the x axis, the band gap energies of the BMT films were obtained. The band gap energy values are 3.73, 3.71, 3.67, and 3.63 eV for Mn: Ti (1/99), Mn: Ti (2/98), Mn: Ti (5/95), and Mn: Ti (10/90) thin films, respectively. This indicates that the band gaps of BMT thin films decrease with increasing Mn contents. This decrease in the energy band gap was already observed in Co-doped SnO_2 and $BaTiO_3$,[4,27] as well as in other transition metal doped oxides.[23] This observation can be explained on the basis of the sp–d exchange interactions between the band electrons and the localized d electrons of the Mn^{4+} ions substituting Ti^{4+} ions. The s–d and p–d exchange interactions give rise to a negative and positive correction to the conduction-band and valence-band edges, respectively.[28] A direct band gap is at the center of the Brillouin zone Γ point in $BaTiO_3$.[25] The states at the bottom of conduction band arise from the threefold degenerate Ti3d t_{2g} orbits, which have lower energy than the twofold degenerate Ti3d e_g orbits at Γ point. Meanwhile, the top of the valence band at the center of Γ consists of O2p orbits, which is consistent with results by X-ray photoemission spectroscopy.[29] The energy gap in $Ba(Ti_{1-x}, Mn_x)O_3$ is determined by the energy difference between the Ti3d orbit

and O2p orbit. The bottom of the conduction bands may gradually declines with increasing Mn content, which results in the decrease in the band gap values. These facts could induce the red shift of E_g values.

4. Conclusions

In conclusion, the optical properties of BMT thin films with various values of x coated on Si(111) substrates by the sol-gel method have been investigated by the spectroscopic ellipsometry in the UV–Vis–NIR region. Using a four-phase fitting model, the spectra of the optical constants have been determined by means of optimization. Our studies show a strong dependence of the optical constants on the Mn/Ti ratio in the deposited films. The refractive index n and the extinction coefficient k increase with increasing Mn content due to the increase in the packing density. On the other hand, the optical band gap energies have been found to decrease from 3.73 to 3.63 eV as the Mn content in the films is increased from 0.01 to 0.10. The properties of E_g are assigned to the contribution of interband transition from valence band O2p levels to conduction band Ti3d levels, which may have potential applications in devices based on ferroelectric thin films.

References

[1] Hu Z, Chu J, Li Y, Jiang K and Zhu Z 2013 *Advances in Ferroelectrics* **6** 109
[2] Zhang T, Ding L H and Zhang W F 2012 *Chin. Phys. B* **21** 047301
[3] Zhang T, Bai Y, Jia C H and Zhang W F 2012 *Chin. Phys. B* **21** 107304
[4] Li Y W, Sun J L, Meng X J, Chu J H and Zhang W F 2004 *Appl. Phys. Lett.* **85** 1964
[5] Gao W L, Deng H M, Huang D J, Yang P X and Chu J H 2011 *J. Phys.: Conf. Ser.* **276** 012163
[6] Zhang T, Zhang W F, Chen Y H and Yin J 2008 *Opt. Commun.* **281** 439
[7] Bin Anooz S, Schwarzkopf J, Dirsyte R, Agócs E, Petrik P, Kwasniewski A, Wagner G and Fornari R 2011 *Thin Solid Films* **519** 3782
[8] Hwang S Y, Kim T J, Yoon J J, Cha Y H, Kim Y D, Seong T G, Kang L S and Nahm S 2011 *J. Nanosci. Nanotechno.* **11** 884
[9] Wu F M, Yang B, Sun E W, Wang Z, Yin Y Q, Pei Y B, Yang W L and Cao W W 2012 *J. Mater. Sci.* **47** 2818
[10] Jiang K, Zhang J Z Yu W L, Hu Z G and Chu J H 2012 *Appl. Phys. A* **106** 877
[11] Deng H, Deng H M, Yang P X and Chu J H 2012 *J. Mater. Sci.: Mater. Electron.* **23** 1215
[12] Dietl T, Ohno H, Matsukura F, Cibert J and Ferrand D 2000 *Science* **287** 1019
[13] Zhang J T, Wu X J and Li Y 2012 *Chin. Phys. B* **21** 010701
[14] Gao S, Lian J, Sun X F, Wang X, Li P and Li Q H 2013 *Chin. Phys. Lett.* **30** 027801
[15] Sio H, Kirillov O A, Dong L, Xu M, Ye P D, Gundlach D and Nguyen N V 2013 *J. Appl. Phys.* **113** 024504
[16] Garcia-Caurel E, De Martino A, Gaston J P and Yan L 2013 *Appl. Spectroscopy* **2** 1
[17] Huang Z M, Zhang Z H, Jiang C P, Yu J, Sun J L and Chu J H 2000 *Appl. Phys. Lett.* **77** 3651
[18] Hu Z G, Wang G S, Huang Z M, Meng X J and Chu J H 2003 *Semicond. Sci. Technol.* **18** 449
[19] Ray J and Hing P 2000 *J. Appl. Phys.* **88** 1008
[20] Jellison G E, Jr Boatner L A, Lowndes D H, McKee R A and Godbole M 1994 *Appl. Opt.* **33** 6053
[21] Raham M M, Yu G L, Krishna K M, Soga T, Wantanable J J, Jimbo T and Umeno M 1998 *Appl. Opt.* **37** 691
[22] Bruggeman D A G 1933 *Ann. Phys. Leipzig* **24** 636
[23] Kirkpatrick S, Gelatt C D and Vecchi M P 1983 *Science* **220** 671
[24] Yang S H, Mo D and Tang X G 2002 *J. Mater. Sci.* **37** 3841
[25] Cai M Q, Yin Z and Zhang M S 2003 *Appl. Phys. Lett.* **83** 2805
[26] Tauc J and Menth A 1972 *J. Non-Cryst. Solids* **8** 569
[27] Ogale S B, Choudhary R J, Buban J P, Lofland S E, Shinde S R, Kale S N, Kulkarni V N, Higgins J, Lanci C, Simpson J R, Browning N D, Das Sarma S, Drew H D, GreeneR L and Venkatesan T 2003 *Phys. Rev. Lett.* **91** 077205
[28] Bouaine A, Brihi N, Schmerber G, Ulhaq-Bouillet C, Colis S and Dinia A 2007 *J. Phys. Chem. C* **111** 2924
[29] Pertosa P, Hollinger G and Michel-Calendini F M 1978 *Phys. Rev. B* **18** 5177